

1 **Diachronous subduction to diamond- and coesite-facies**
2 **conditions in the Kokchetav massif**

3

4 *Daniela Rubatto⁽¹⁾, Andrey Korsakov⁽²⁾, Jörg Hermann⁽¹⁾, Nikolai L. Dobretsov⁽²⁾*

5

6 *(1) Research School of Earth Sciences, The Australian National University, Canberra 0200,*
7 *Australia.*

8 *(2) Institute of Geology and Mineralogy, Siberian Branch of the RAS, Novosibirsk 630090, Russia*

9

10 **Abstract**

11 The absolute and relative time of subduction of rocks is crucial information for
12 subduction-exhumation models. We investigated the timing of subduction in one
13 of the oldest ultra-high pressure (UHP) localities worldwide: the Kokchetav massif
14 in Kazakhstan. SHRIMP ion microprobe dating of monazite from coesite-bearing
15 micaschists of the Kulet unit indicates that subduction occurred between ~500-
16 520 Ma. This new data provides evidence that the Kulet unit underwent UHP
17 metamorphism 10-15 Ma later than the diamond-facies rocks in the nearby
18 Kumdy-Kol unit. This time constrain excludes models that argue for a
19 simultaneous evolution of coesite- and diamond-facies rocks, it suggest that
20 subduction continued well after continental crust was involved, and that
21 exhumation was not initiated by a single event such as slab break-off. The
22 dynamic of this UHP massif also indicates that Cambrian tectonic was similar to
23 that of recent orogenic belts.

24

25 **Introduction**

26 The study of crustal rocks that underwent UHP conditions, i.e. subduction to
27 the coesite and diamond stability fields (> 90 Km depth) offers a unique insight
28 into the deep Earth and the tectonic processes of subduction and exhumation. It
29 has been proposed that the first occurrence of UHP metamorphism defines the
30 time of onset of modern cold subduction on Earth (Brown, 2006). The Kokchetav
31 massif in Kazakhstan contains some of the oldest known UHP rocks, which
32 reached diamond-facies conditions indicating subduction to at least 150 km
33 depth, at ~530 Ma (Claoué-Long et al., 1991; Hermann et al., 2001; Katayama et
34 al., 2001). These rocks therefore provide a rare opportunity to study fundamental
35 processes at the onset of modern plate tectonics. In addition to determining the
36 P-T conditions recorded by the rocks, the timing of subduction and exhumation is
37 crucial to constrain the tectonic processes responsible for UHP metamorphism.
38 For example, it has been shown in the Kokchetav massif and in the Alps that
39 exhumation can be as fast as subduction, acting at rates of cm/year (Hermann et
40 al., 2001; Rubatto and Hermann, 2001). This provides strong evidence that
41 tectonic processes and not erosion drives exhumation, and is an important
42 constraint for exhumation models. A number of different tectonic models have
43 been proposed to explain how crustal rocks can be subducted to, and exhumed
44 from, such great depth (e.g. Chemenda et al., 1996; Cloos, 1993; Gerya et al.,
45 2002; Kurz and Froitzheim, 2002). The detailed knowledge of the timing of UHP
46 metamorphism is crucial to evaluate these different models.

47 The UHP rocks of the Kokchetav massif are contained within two separate
48 zones: a diamond-bearing unit and a coesite-bearing unit. While there are
49 abundant age data for the diamond-bearing rocks, few age constraints exist for
50 the coesite-bearing unit, where the temperatures are too high for Ar-Ar dating but
51 too low to produce metamorphic zircon. In this paper we show that in Ca-poor
52 rock types of the coesite bearing unit, monazite is stable up to UHP conditions.
53 Such monazite is dated using SHRIMP and provides evidence that UHP
54 metamorphism is diachronous in the coesite and diamond units. This time
55 constraint has a strong bearing on the type of tectonic model applicable to this
56 area and is comparable to what has been documented in younger collisional
57 belts such as the Alps.

58

59 **Two contrasting UHP domains**

60 The Kokchetav massif is located in the central part of the Eurasian craton and
61 extends NW-SE over 150 km with a thickness of 20 km. This HP-UHP belt is
62 composed of several metamorphic units derived from Precambrian protoliths,
63 overlain by Devonian volcanoclastic and Carboniferous-Triassic shallow-water
64 deposits, and intruded by Ordovician granites and gabbros (Dobretsov et al.,
65 1995; Maruyama and Parkinson, 2000). Two contrasting UHP domains have
66 been described in the Kokchetav massif: the diamond-bearing unit at Kumdy-Kol
67 and the nearby coesite-bearing unit at Kulet (Dobretsov et al., 1998; Theunissen
68 et al., 2000; Udovkina, 1985). There is mounting evidence of different P-T
69 conditions in the two areas with $P = 4-6$ GPa and $T = 950-1000^{\circ}\text{C}$ in Kumdy-Kol

70 (Hermann et al., 2001; Maruyama and Parkinson, 2000; Shatsky et al., 1995;
71 Zhang et al., 1997), versus $P = 3.4-3.6$ GPa and $T = 720-760^{\circ}\text{C}$ in Kulet
72 (Parkinson, 2000).

73 Two alternative models have been proposed for the juxtaposition of these
74 UHP domains. The *extrusion wedge* model suggests that the two units were
75 exhumed simultaneously by the same process and stacked together during
76 exhumation (Maruyama and Parkinson, 2000). In contrast the *megamelange*
77 model emphasizes different evolutions and thus exhumation processes for the
78 diamond- and the coesite-bearing unit (Dobretsov et al., 1995; Shatsky et al.,
79 1995; Theunissen et al., 2000). Still lacking is the time information in order to
80 assess whether the exhumation of these UHP units is coupled or decoupled.
81 There are several studies concerning the age of UHP metamorphism in the
82 diamond-bearing rocks (e.g. Claoué-Long et al., 1991; Hermann et al., 2001;
83 Katayama et al., 2001; Shatsky et al., 1999), which reached peak UHP at ~530
84 Ma, and then were quickly decompressed to granulite and then amphibolite-
85 facies conditions (~525 Ma). The diamond-bearing rocks cooled below the
86 closure of Ar-Ar system in mica at 515-517 Ma (Shatsky et al., 1999). In contrast,
87 only Ar-Ar ages are available for the coesite-bearing rocks of Kulet: they scatter
88 between 565-520 Ma (Theunissen et al., 2000) and ~500 Ma (Hacker et al.,
89 2003). These ages leave the possibility open that the two UHP units were
90 exhumed at different times.

91

92 **Sample and monazite description**

93 We have investigated in detail two garnet-bearing micaschists from the
94 coesite-facies Kulet area, which contain different types of monazite. Sample
95 Ku98-12 is a coarse-grained and strongly foliated micaschist consisting of garnet,
96 quartz, phengite, kyanite, rutile, monazite and rare zircon. Garnet forms
97 dispersed porphyroblasts up to 1 cm in diameter with common rutile and rare
98 large polycrystalline quartz inclusions. Monazite inclusions occur throughout the
99 garnet and are associated to chlorite, apatite and kyanite (Fig. 1a). In garnet, Mn,
100 Y and HREE strongly decrease from core to rim whereas Mg# [$Mg/(Mg+Fe)$]
101 increases in agreement with a prograde growth (Fig. DR1 and Parkinson, 2000).
102 The pyrope-rich garnet rims are in textural equilibrium with kyanite and large
103 oriented phengite (Si=3.38 pfu, 0.5 wt% TiO₂, Fig. DR2a) that occasionally
104 contain monazite inclusions. Large phengite grains are surrounded by smaller
105 laths (Si=3.28 pfu, 0.6 wt% TiO₂) indicating recrystallization during
106 decompression. Both types of phengite recrystallized at the margins to fine-
107 grained phengite (Si=3.21 pfu, 0.55 wt% TiO₂), which in turn is partly replaced by
108 even finer grained muscovite (Si=3.10 pfu, 0.3 wt% TiO₂) that coexists with
109 biotite. Biotite also replaces garnet rims and occasionally contains monazite
110 inclusions. The textural relations and mineral compositions suggest that this
111 micaschist documents a prograde, peak and several retrograde metamorphic
112 stages, during all of which monazite appears to be stable.

113 Sample K26C is a whiteschist mainly composed of quartz and garnet with
114 phengite (Si=3.5 pfu, 0.2 wt% TiO₂) defining a foliation. Euhedral garnet
115 porphyroblasts, similar to those described by Parkinson (2000), contain
116 inclusions of monocrystalline quartz in the core and typical polycrystalline
117 palisade- or mosaic-quartz aggregates surrounded by weak radial cracks in the
118 rim. Large anhedral garnet porphyroblasts contain inclusions of polycrystalline
119 quartz with radial cracks and coesite relics. Fresh coesite is still locally preserved
120 (Shatsky et al., 1998). In contrast to the first sample, where large monazite grains
121 were found, monazite is present only in small (<100 μm) symplectite-like
122 aggregates with apatite and phengite (Fig. 1b). Such symplectites are found
123 within the rim of the large garnet porphyroblasts and in the matrix. The varying
124 proportions of monazite (30-80%) and apatite (10-55%) in the symplectites
125 suggest that the precursor mineral likely was a solid solution between apatite and
126 monazite end-members. Similar textures (apatite-monazite symplectites after
127 bearthite) have been observed in UHP whiteschists (Scherrer et al., 2001) and
128 micaschists (Hermann pers. comm.) from the Dora Maira (Italy) and are
129 interpreted to form during decompression.

130 The presence of coesite and coesite pseudomorphs provide evidence that the
131 rocks experienced UHP peak conditions which, based on peak mineral
132 compositions, are estimated to be ~2.8 GPa, ~680°C using the calibrations of
133 Krogh Ravna and Terry (2004) and Green and Hellman (1982), respectively. This
134 is slightly lower than what has been reported in the detailed study of Parkinson
135 (2000), who obtained 720-760°C and 3.4-3.6 GPa for the peak conditions of the

136 Kulet whiteschists. The several retrograde stages documented by phengite are in
137 agreement with an initial near isotherm decompression stage to about 1.8 GPa,
138 640°C followed by decompression and cooling, as outlined by Parkinson (2000).

139

140 **Monazite U-Pb geochronology**

141 U-Th-Pb analyses were obtained for monazite grains separated from
142 micaschist Ku98-12 and for monazite contained in the symplectites of micaschist
143 K26C. This latter was analysed directly in thin section.

144 Back-scattered electron images (Fig. 1c-e) of monazite from sample Ku98-12
145 reveal a weak zoning that is organised in a core-rim (core brighter than rim) or
146 mosaic-like texture. Monazite contains inclusions of phengite with variable
147 composition (Fig. DR2a), chlorite, apatite, zircon and rutile. Inclusions are equally
148 distributed between core and rim and the inclusions, particularly phengite, are
149 found across the core-rim boundary (e.g. Fig. 1d). This supports the textural
150 observations that monazite was stable over a large portion of the metamorphic
151 history of the sample.

152 SHRIMP analyses yielded $^{206}\text{Pb}/^{238}\text{U}$ ages between 488 and 529 Ma (Table
153 DR1 and Fig. 2), with a scatter of data above analytical uncertainty (507 ± 3 Ma
154 $\text{MSWD} = 7.3$, $N = 54$, or $\text{MSWD} = 5.2$ excluding three extreme values). The
155 scatter of ages somewhat correlates with the core-rim structure seen in BSE; i.e.
156 within a crystal, cores are older or equal in age to the rims, but never younger
157 than the rims (Fig. 1c-e). However, throughout the sample core and rim ages
158 vary significantly and overlap (~496-529 Ma and 491-520 Ma, respectively).

159 There is no clear correlation between age and monazite composition as
160 measured by EMP analysis close to the SHRIMP pits. Older monazite domains
161 have a weak tendency to higher Y and Gd contents (Fig. DR2b). However,
162 overall a limited chemical variation is observed in the monazite grains (Fig.
163 DR3a). This information can be used to compare monazite to garnet growth by
164 using empirical trace element partitioning between monazite and the different
165 garnet growth zones (e.g. Hermann and Rubatto, 2003). The garnet in sample
166 Ku98-12 has a bell-shaped major and trace element zoning that indicates
167 prograde growth culminating in a rim with high Mg#, low Mn, Y and REE. The
168 HREE distribution coefficients between the monazite composition (either core or
169 rim) and the garnet rim composition decrease constantly from Dy (30-75) to Lu
170 (0.8-2.2) (Fig. DR3). Similar values were reported for monazite/garnet equilibrium
171 partitioning in granulites (e.g. Buick et al., 2006; Hermann and Rubatto, 2003;
172 Rubatto et al., 2006). The partitioning of HREE between monazite, and the
173 garnet core is at least an order of magnitude lower and far from any equilibrium
174 partitioning reported. This provides evidence that the monazite dated in sample
175 Ku98-12 is in chemical equilibrium with the garnet rim. Garnet break down is
176 restricted to the last retrograde event, where a fine biotite rim forms around
177 garnet. Therefore the dated monazite must have formed in the period between
178 the last stage of prograde garnet growth and the late retrogression when biotite
179 formed.

180 Some of the old monazite domains have inclusions of chlorite, which occurs as
181 prograde mineral enclosed in garnet, but is not stable in the peak assemblage.

182 This suggests that at least some of the older monazite may have formed before
183 the metamorphic peak. The composition of phengite inclusions in monazite spans
184 the entire range documented in the rock (Si=3.1-3.4 pfu, Fig. DR2a), indicating
185 that monazite recrystallization/formation occurred during peak and several
186 retrograde stages. However, there is no systematic relationship between Si-
187 content of the inclusion and the age of the monazite domain (Fig. DR2c). For
188 example phengite with 3.4 pfu of Si is present as inclusion in a 526 Ma cores as
189 well as in a 491 Ma domain.

190 The combined evidence from monazite textures, trace element composition,
191 inclusion assemblage and ages suggests that the age spread is geologically
192 significant and indicates growth/recrystallization of monazite over a period of
193 time. The youngest and oldest statistically consistent (MSWD ~ 1) group of
194 analyses within the age spread observed are at 497 ± 2 Ma and 522 ± 2 Ma (Fig.
195 2). These values can be taken as bracketing the ~25 Ma time span of monazite
196 growth between prograde-peak metamorphic conditions and amphibolite facies
197 retrogression.

198 SHRIMP U-Pb analyses on micaschist K26C was done with a small spot size
199 (10-15 micron diameter) to maximise the chances to get clean monazite
200 analyses. Filtering the data according to the percent of monazite versus other
201 phases in the analysis (see analytical methods in DR) returns a main group with
202 an average $^{206}\text{Pb}/^{238}\text{U}$ age of 508 ± 6 Ma (MSWD 0.67, N = 7, Table DR2) and an
203 identical concordia age (Fig. 2). In this sample, the monazite-forming reaction is
204 likely to be the breakdown of precursor bearthite. The obtained age thus dates

205 this reaction, which is related to the exhumation of the UHP rocks, although the
206 exact P-T conditions of the reaction cannot be established. The HP minerals
207 texturally associated to the symplectites indicate that the reaction occurred still at
208 relatively HP conditions.

209

210 **Monazite versus zircon behaviour during deep subduction**

211 Zircon is known to react in various ways during deep subduction, from
212 recrystallization in sub-solidus conditions under the influence of fluids to new
213 growth favoured by melting (Rubatto and Hermann, 2007). An example of new
214 zircon formation at UHP is represented by zircon found in the Kokchetav
215 diamond-bearing unit of Kumdy-Kol (Hermann et al., 2001; Katayama et al.,
216 2001). In contrast, the zircons contained in the coesite-bearing rocks of Kulet do
217 not show any metamorphic domains of appreciable size (> a few μm). The
218 difference in behaviour is likely due to the presence of a melt in the diamond-
219 bearing unit, which favoured dissolution-precipitation of zircon. The coesite-
220 bearing rocks experienced lower metamorphic conditions below the pelite solidus
221 (Fig. 3, Nichols et al., 1994), conditions at which metamorphic zircon formation
222 can be very limited and restricted to zones rich in fluids (see a review in Geisler
223 et al., 2007; Rubatto and Hermann, 2007).

224 This study shows that monazite can be used to date UHP rocks in conditions
225 not favourable to metamorphic zircon. As demonstrated in regional metamorphic
226 sequences, monazite forms and/or recrystallizes at lower grade than zircon.
227 Monazite is expected to be present at HP and UHP conditions only in Ca-poor

228 rocks, where the stability of the most common LREE mineral, allanite, is
229 suppressed (Hermann, 2002). We report here one of the first occurrences of
230 UHP monazite (see also Terry et al., 2000). Finger and Krenn (2007)
231 documented in detail HP monazite from a Al-rich, Ca-poor rock, in which
232 monazite is stable during prograde, peak (26 ± 3 kbar, $830\pm 30^\circ\text{C}$) and retrograde
233 conditions. That HP monazite is characterised by high Sr contents (Sr 0.85-1.7
234 wt%) indicating formation after breakdown of plagioclase. This chemical criterion
235 is however not valid for the Kokchetav monazite (Sr 500-1000 ppm) because
236 these Ca-poor micaschist do not contain plagioclase even at low pressures. In
237 rocks richer in calcium, allanite or bearthite are the stable LREE phases
238 (Hermann, 2002; Scherrer et al., 2001), and monazite will form during the
239 decompressional break down of these phases. In either case, dating of monazite
240 can yield time constraints on the peak and/or exhumation history of UHP rocks.

241

242 **Age significance and implications**

243 The new age data permit to construct a P-T-time diagram for the coesite-
244 bearing UHP unit that can be compared to the known evolution of the diamond-
245 bearing unit (Fig. 3). Based on texture, trace element composition and inclusions
246 in monazite it is concluded that the pressures peak was reached at ~ 520 - 515 Ma.
247 Decompression is dated by the formation of monazite symplectites in sample
248 Ku26C at 508 ± 6 Ma. This implies that the coesite-bearing unit underwent UHP
249 metamorphism when the diamond unit was already exhumed at mid crustal levels
250 (Fig. 3). The monazite ages cannot be reconciled with the scattering Ar-Ar data of

251 Theunissen et al. (2000) who obtained biotite and phengite ages of ~520 Ma
252 (including an age of 519 ± 2 Ma for our sample Ku98-12), but also an older
253 muscovite age of 565 ± 2 Ma for sample K26C. The monazite data fit well the
254 internally consistent Ar-Ar ages of Hacker et al. (2003) on micas at ~ 500 Ma.
255 There was thus a time lag of circa 15 Ma between the metamorphic evolution of
256 the diamond and coesite-bearing units. Although the P-T evolution of the
257 diamond-facies and coesite-facies rocks are comparable from amphibolite facies
258 onward (Fig. 3), they are separated in time and thus juxtaposition of the two units
259 must have occurred once the rocks were exhumed to mid crustal levels.

260 This timing relationship has important implications on the tectonic model for
261 the UHP subduction and exhumation of the Kokchetav massif. Diachronous
262 evolution of the two UHP units is incompatible with the *extrusion-wedge* model
263 (Maruyama and Parkinson, 2000), but the *megamelange* model could
264 accommodate this time constraints (Dobretsov et al., 1995). From our data it can
265 also be added that continental subduction of the Kumdy-Kol unit to diamond-
266 facies conditions did not mark the transition from subduction to collision, because
267 UHP metamorphism occurred in the Kulet micaschists 15 Ma later. Therefore,
268 classical models where continental collision leads to cessation of subduction and
269 initiates exhumation (e.g. Chemenda et al., 1996; Cloos, 1993) cannot be applied
270 to the Kokchetav massif. It also renders unrealistic models where a single event
271 such as collision or slab break-off initiate exhumation (e.g. Hermann et al., 2001;
272 von Blanckenburg and Davies, 1995). On the other hand, the obtained ages
273 would be consistent with the subduction channel models of Gerya et al. (2002).

274 This represents an exemplar case where geochronology can directly assist
275 tectonics in defining a workable subduction-exhumation model.

276 Diachronous subduction and exhumation is well documented in the Western
277 Alps. There is evidence for different units undergoing similar subduction
278 conditions at different times (e.g. Rubatto et al., 1998), and a recent model
279 proposes exhumation of diachronous slices of HP rocks equilibrated at different
280 depths inside a subduction channel (Federico et al., 2007). We can thus draw a
281 similarity between the Cambrian tectonic represented in the Kokchetav massif
282 and the Paleogene Alpine orogeny. This represents supporting evidence that not
283 only modern cold subduction (Brown, 2006), but also complex and diachronous
284 exhumation, has been acting since at least the early Paleozoic era.

285

286

287 **REFERENCES**

288 Brown, M., 2006, Duality of thermal regimes is the distinctive characteristic of plate
289 tectonics since the Neoproterozoic: *Geology*, v. 34, p. 961-964.

290 Buick, I.S., Hermann, J., Williams, I.S., Gibson, R., and Rubatto, D., 2006, A SHRIMP U-
291 Pb and LA-ICP-MS trace element study of the petrogenesis of garnet-cordierite-
292 orthoamphibole gneisses from the Central Zone of the Limpopo Belt, South
293 Africa.: *Lithos*, v. 88, p. 150-172.

294 Chemenda, A.I., Mattauer, M., and Bokun, A.N., 1996, Continental subduction and a
295 mechanism for exhumation of high-pressure metamorphic rocks: new modelling
296 and field data from the Oman: *Earth and Planetary Science Letters*, v. 143, p.
297 173-182.

298 Claoué-Long, J.C., Sobolev, N.V., Shatsky, V.S., and Sobolev, A.V., 1991, Zircon
299 response to diamond-pressure metamorphism in the Kokchetav massif, USSR:
300 Geology, v. 19, p. 710-713.

301 Cloos, M., 1993, Lithospheric buoyancy and collisional orogenesis: Subduction of oceanic
302 plateaus, continental margins, island arcs, and seamounts: Geological Society of
303 America Bulletin, v. 105, p. 715-737.

304 Dobretsov, N.L., Sobolev, N.V., Shatsky, V.S., Coleman, R.G., and Ernst, W.G., 1995,
305 Geotectonic evolution of diamondiferous paragneisses of the Kokchetav
306 complex, Northern Kazakhstan - the geological enigma of ultrahigh-pressure
307 crustal rocks within Phanerozoic foldbelts: Island Arc, v. 4, p. 267-279.

308 Dobretsov, N.L., Theunissen, K., and Smirnova, L.V., 1998, Structural and geodynamic
309 evolution of diamond-bearing metamorphic rocks of Kokchetav massif,
310 Kazakhstan: Geologiya i Geofizika, v. 39, p. 1645-1666.

311 Federico, L., Crispini, L., Scambelluri, M., and Capponi, G., 2007, Ophiolite mélange
312 zone records exhumation in a fossil subduction channel: Geology, v. 35, p. 499-
313 502.

314 Finger, F., and Krenn, E., 2007, Three metamorphic monazite generations in a high-
315 pressure rocks from the Bohemian Massif and the potentially important role of
316 apatite in stimulating polyphase monazite growth along a PT loop: Lithos, v. 95,
317 p. 103-115.

318 Geisler, T., Schaltegger, U., and Tomaschek, F., 2007, Re-equilibration of zircon in
319 aqueous fluids and melts: Elements, v. 3, p. 43-50.

320 Gerya, T., Stockhert, B., and Perchuk, A., 2002, Exhumation of high-pressure
321 metamorphic rocks in a subduction channel: A numerical simulation: Tectonics, v.
322 21, p. Art. No. 1056.

323 Green, D.H., and Hellman, P.L., 1982, Fe-Mg partitioning between coexisting garnet and
324 phengite at high pressure, and comments on a garnet-phengite geothermometer:
325 *Lithos*, v. 15.

326 Hacker, B.R., Calvert, A., Zhang, R.Y., Ernst, W.G., and Liou, J.G., 2003, Ultrarapid
327 exhumation of ultrahigh-pressure diamond-bearing metasedimentary rocks of the
328 Kokchetav Massif, Kazakhstan?: *Lithos*, v. 70, p. 61-75.

329 Hermann, J., 2002, Allanite: Thorium and light rare earth element carrier in subducted
330 crust: *Chemical Geology*, v. 192, p. 289-306.

331 Hermann, J., and Rubatto, D., 2003, Relating zircon and monazite domains to garnet
332 growth zones: age and duration of granulite facies metamorphism in the Val
333 Malenco lower crust: *Journal of Metamorphic Geology*, v. 21, p. 833-852.

334 Hermann, J., Rubatto, D., Korsakov, A., and Shatsky, V.S., 2001, Multiple zircon growth
335 during fast exhumation of diamondiferous, deeply subducted continental crust
336 (Kokchetav massif, Kazakhstan): *Contributions to Mineralogy and Petrology*, v.
337 141, p. 66-82.

338 Katayama, I., Maruyama, S., Parkinson, C.D., Terada, K., and Sano, Y., 2001, Ion micro-
339 probe U-Pb zircon geochronology of peak and retrograde stages of ultrahigh-
340 pressure metamorphic rocks from the Kokchetav massif, northern Kazakhstan:
341 *Earth and Planetary Science Letters*, v. 188, p. 185-198.

342 Krogh Ravn, E.J., and Terry, M.P., 2004, Geothermobarometry of UHP and HP
343 eclogites and schists - an evaluation of equilibria among garnet-clinopyroxene-
344 kyanite-phengite-coesite/quartz: *Journal of Metamorphic Geology*, v. 22.

345 Kurz, W., and Froitzheim, N., 2002, The exhumation of eclogite-facies metamorphic
346 rocks - a review of models confronted with examples from the Alps: *International
347 Geology Review*, v. 44, p. 702-743.

348 Maruyama, S., and Parkinson, C.D., 2000, Overview of the geology, petrology, and
349 tectonic framework of the UP-UHPM Kokchetav Massif, Kazakhstan: *Island Arc*,
350 v. 9, p. 439-455.

351 Nichols, G.T., Wyllie, P.J., and Stern, C.R., 1994, Subduction zone melting of pelagic
352 sediments constrained by melting experiments: *Nature*, v. 371, p. 785-788.

353 Parkinson, C.D., 2000, Coesite inclusions and prograde compositional zonation of
354 garnet in whiteschists of the HP-UHP Kokchetav massif, Kazakhstan, a record of
355 progressive UHP metamorphism: *Lithos*, v. 52, p. 215-233.

356 Rubatto, D., Gebauer, D., and Fanning, M., 1998, Jurassic formation and Eocene
357 subduction of the Zermatt - Saas-Fee ophiolites: Implications for the geodynamic
358 evolution of the Central and Western Alps: *Contributions to Mineralogy and*
359 *Petrology*, v. 132, p. 269-287.

360 Rubatto, D., and Hermann, J., 2001, Exhumation as fast as subduction?: *Geology*, v. 29,
361 p. 3-6.

362 —, 2007, Zircon behaviour in deeply subducted rocks: *Elements*, v. 3, p. 31-35.

363 Rubatto, D., Hermann, J., and Buick, I.S., 2006, Temperature and bulk composition
364 control on the growth of monazite and zircon during low-pressure anatexis
365 (Mount Stafford, central Australia): *Journal of Petrology*, v. 47, p. 1973-1996.

366 Scherrer, N., Gnos, E., and Chopin, C., 2001, A retrograde monazite-forming reaction in
367 bearthite-bearing high-pressure rocks: *Schweizerische Mineralogische und*
368 *Petrographische Mitteilungen*, v. 81.

369 Shatsky, V.S., Jagoutz, E., N.V., S., Kozmenko, O.A., Parkhomenko, V.S., and Troesch,
370 M., 1999, Geochemistry and age of ultrahigh pressure metamorphic rocks from
371 the Kokchetav massif (Northern Kazakhstan): *Contributions to Mineralogy and*
372 *Petrology*, v. 137, p. 185-205.

373 Shatsky, V.S., Rylov, G.M., Efimova, E.S., Corte, K., and Sobolev, N.V., 1998,
374 Morphology and real structure of microdiamonds from metamorphic rocks of the
375 Kokchetav massif, kimberlites, and alluvial placers: *Geologiya i Geofizika*, v. 39.
376 Shatsky, V.S., Sobolev, N.V., and Vavilov, M.A., 1995, Diamond-bearing metamorphic
377 rocks of the Kokchetav massif (Northern Kazakhstan), *in* Coleman, R.G., and
378 Wang, X., eds., *Ultrahigh pressure metamorphism*: Cambridge, Cambridge
379 University Press, p. 427-455.

380 Terry, M.P., Robinson, P., Hamilton, M.A., and Jercinovic, M.J., 2000, Monazite
381 geochronology of UHP and HP metamorphism, deformation, and exhumation,
382 Nordoyane, Western Gneiss region, Norway: *American Mineralogist*, v. 85, p.
383 1651-1664.

384 Theunissen, K., Dobretsov, N.L., Korsakov, A., Travin, A., Shatsky, V.S., Smirnova, L.,
385 and Boven, A., 2000, Two contrasting petrotectonic domains in the Kokchetav
386 megamelange (north Kazakhstan): Difference in exhumation mechanisms of
387 ultrahigh-pressure crustal rocks, or a result of subsequent deformation?: *Island
388 Arc*, v. 9, p. 284-303.

389 Udovkina, N.G., 1985, *Eclogites of the USSR*: Moscow, Nauka Press.

390 von Blanckenburg, F., and Davies, J.H., 1995, Slab break-off: A model for syncollisional
391 magmatism and tectonics in the Alps: *Tectonics*, v. 14, p. 120-131.

392 Zhang, R.Y., Liou, J.G., Coleman, R.G., Ernst, W.G., Sobolev, A.V., and Shatsky, V.S.,
393 1997, Metamorphic evolution of the diamond-bearing and associated rocks from
394 the Kokchetav massif, northern Kazakhstan: *Journal of Metamorphic Geology*, v.
395 15, p. 479-496.

396

397 **FIGURE CAPTIONS**

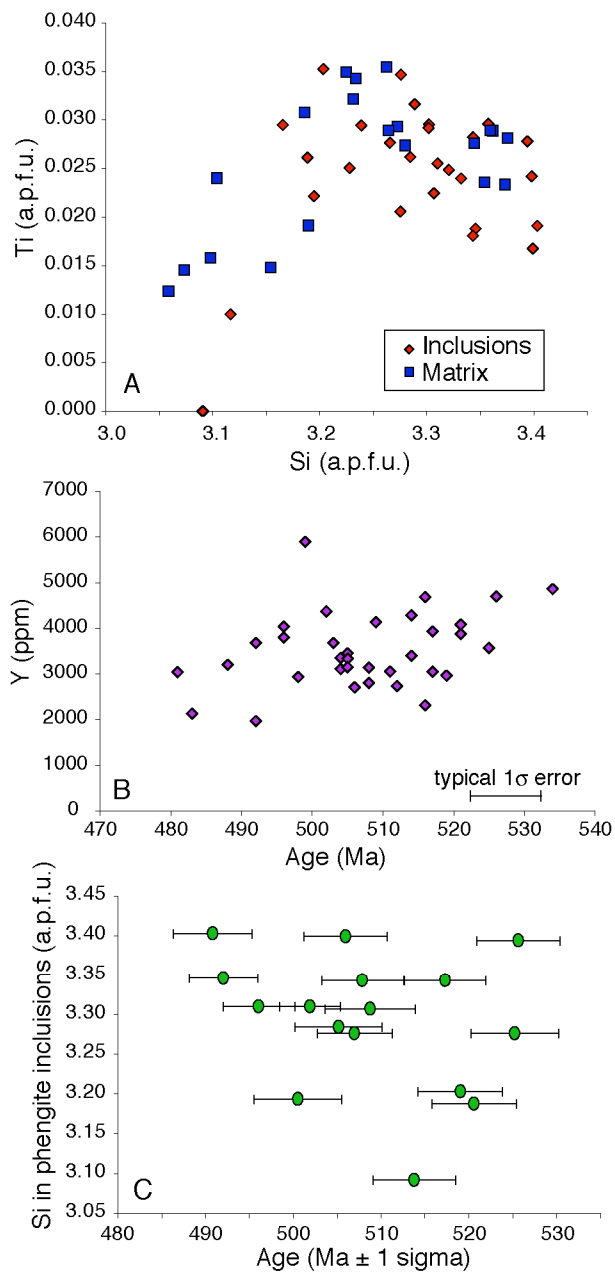
398 Fig. 1. Back-scattered electron images of monazite textural relationships. A)
399 Composite inclusion in garnet consisting of monazite, apatite, kyanite and chlorite
400 from sample Ku98-12. B) Symplectite of monazite, apatite and phengite, likely
401 formed from decompression of bearthite in sample K26C. C-E) High contrast
402 images of monazite crystals in sample Ku98-12. Note the core-rim structure and
403 the inclusions of phengite with different Si contents. Circles mark SHRIMP pits for
404 which $^{206}\text{Pb}/^{238}\text{U}$ ages (Ma ± 1 sigma) are reported. Y contents from EMP
405 analysis of the same domain are given in ppm.

406

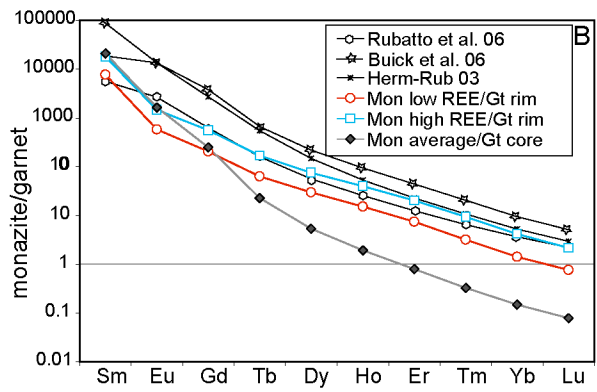
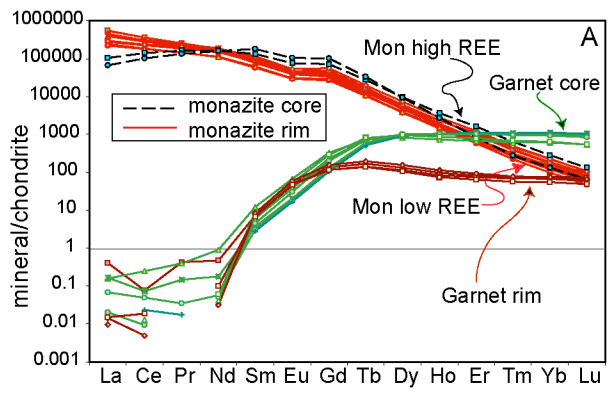
407 Fig. 2. Monazite U-Pb geochronology. A) Plot of $^{206}\text{Pb}/^{238}\text{U}$ ages for sample
408 Ku98-12 showing the wide age range. The statistically consistent (MSWD~1)
409 older and younger age group are reported. B) Concordia diagram for U-Pb
410 analyses of monazite symplectites in sample K26C. The Concordia age reported
411 in the box is represented by the darker ellipse. Average ages are at 95% c.l..

412

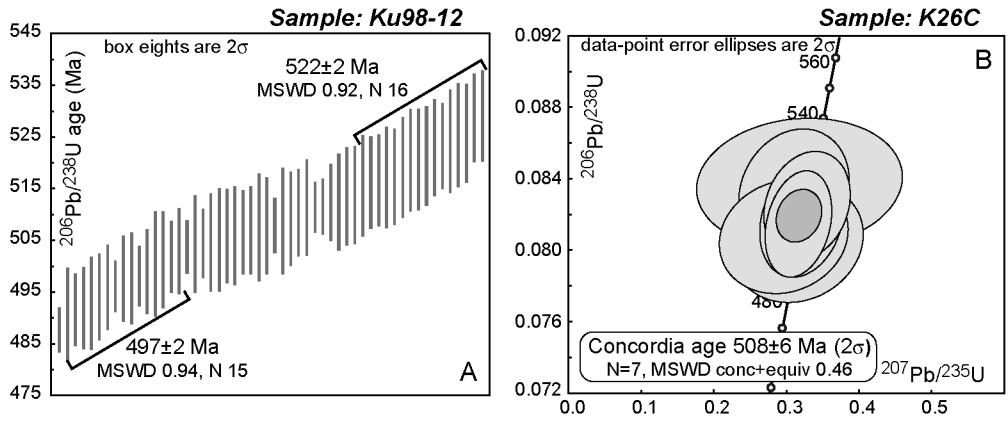
413 Fig. 3. P-T-time path for the two UHP units of the Kokchetav massif. Ages are
414 given in Ma and are U-Pb on zircon (Kumdy-Kol) or monazite (Kulet) and Ar-Ar
415 on mica (in italics). The P-T-time path for Kumdy-Kol is after Hermann et al.
416 (2001) and references therein. For Kulet, the P-T estimates are from this work
417 (thick black line) and Parkinson (2000) (thin black dashed line). Kulet U-Pb ages
418 are from this work (tw), and Ar-Ar ages are from Hacker et al. (2003). Wet solidus
419 from Nichols et al. (1994). See text for discussion.



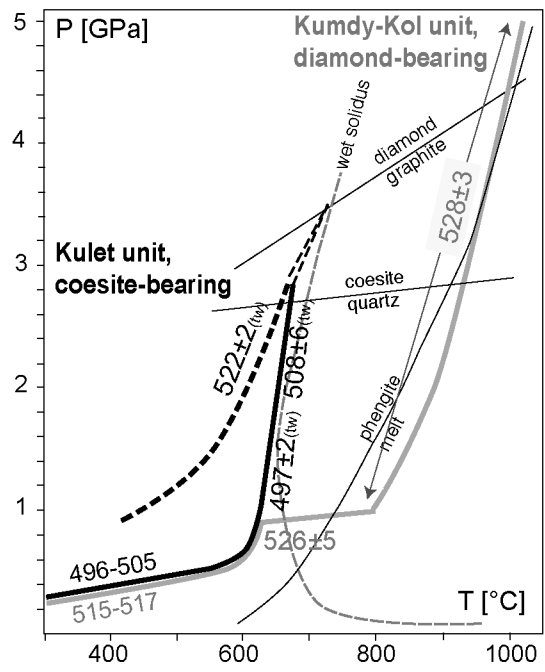
Rubatto et al. Data Repository, Fig. 2



Rubatto et al., Data Repository Fig. 3



Rubatto et al., Figure 2



Rubatto et al., Fig. 3.